

DPL non-Fourier heat transfer modelling in porous materials and validation using IR measurement

by M. Strąkowska*, G. De Mey** and B. Więcek*

* Lodz University of Technology, 90-924, 116 Żeromskiego Str., Lodz, Poland, maria.strakowska@p.lodz.pl

**University of Gent, 9052, 126 Technologiepark-Zwijnaarde, Gent, Belgium

Abstract

Dual Phase Lag (DPL) thermal modelling is of interest to many researchers, but most focus solely on modelling without validating it through the convincing experiments, in particular using IR radiation measurements. Measurement such phenomenon is challenging due to the small temperature signals of objects under observation. We propose a novel method using infrared thermography measurements to derive the thermal impedance of the object by analysing the fundamental harmonics of the thermal response. This approach enables the determination of the thermal impedance of the measured object and confirms the presence of the dual phase lag phenomenon in porous materials. Furthermore, we aim to validate the assumption that DPL heat conduction can be interpreted as the heat transfer in a material whose thermal conductivity depends on frequency.

1. Introduction

Experimental validation of Dual Phase Lag heat transfer model is still a very challenging task. This non-Fourier heat transfer phenomenon was observed, among others, in porous material such as wet sand and tissues [1-17]. The problem is that the DPL effect is revealed at very beginning of the transient state while the object is either heated up or cooled down. Moreover, in transient states, the temperature deviates very little from the monotonic increase or decrease typical of Fourier-Kirchhoff heat transfer, making these changes difficult to measure [1]. The DPL heat transfer is described by 2 thermal delay times (τ_q and τ_T) that redefines the heat flux q [1, 2, 3].

$$q(x, t + \tau_q) = -k \frac{\partial T(x, t + \tau_T)}{\partial x} \quad (1)$$

where k is thermal conductivity.

By applying the Taylor series, the eq. (1) can be approximated by:

$$q(x, t) + \tau_q \frac{\partial q(x, t)}{\partial t} \approx -k \left[\frac{\partial}{\partial x} \left(T(x, t) + \tau_T \frac{\partial T(x, t)}{\partial t} \right) \right] \quad (2)$$

Further simplification can hide derivation in time by using Laplace transform.

$$q(x, s)(1 + s\tau_q) = -k \frac{\partial T}{\partial x} (1 + s\tau_T) \quad (3)$$

where $s=j\omega$.

Eq. (3) can be interpreted as a redefinition of heat flux and thermal conductivity. Taking into account the Fourier's law of heat transfer, DPL approach can be interpreted by introducing thermal conductivity \tilde{k} , which is no more a real value, but a complex one, depending on frequency [16,17].

$$q(x, s) = -\tilde{k} \frac{\partial T}{\partial x} = -k \frac{1+s\tau_T}{1+s\tau_q} \frac{\partial T}{\partial x} \quad (4)$$

In consequence, the thermal conductivity defined in this way contributes not only to the amount of heat transferred through the material, but also it has an impact on phase shift between power and temperature in the transient and AC heat transfer. In the literature, there still ongoing discussion on the thermodynamic consistency of DPL thermal modelling [1-18]. The authors confirm the better agreement of DPL approach with results obtained in experiments in contrast to hyperbolic heat conduction. On the other hand, there are various theoretical investigations showing the simulation results for 2 different cases: either $\tau_T \geq \tau_q$ or $\tau_T < \tau_q$ [2,3,4,8,18]. If $\tau_T \geq \tau_q$ is valid, the diffusive nature of heat transfer dominates. Mathematically, it is manifested by the first order time derivative of temperature in the heat transfer equation. In the opposite case ($\tau_T < \tau_q$), the heat propagates in solids as a wave. In the equation, the second order derivative of temperature in time appears formulating the hyperbolic heat transfer. Mathematically, the very high speed of waves at high frequency is possible, what is physically not accepted [18]. From the physical point of view, it is difficult to explain such phenomenon, especially in macro scale. The wave effect of heat propagation was observed in nanostructures excited by ultra-short heat injection pulses, e.g. delivered by femtosecond lasers [1]. In metals for example, the time delays τ_T and τ_q are of the order of picoseconds, but they still preserve the relation $\tau_T > \tau_q$ ensuring the diffusive character of heat transfer [1,2]. The DPL model allows for simultaneous balancing of hyperbolic and diffusive contribution in the heat transfer. In general, it can provide a good match to experimental results, however the question on the physical aspect of the model still remains.

In this research we deal with macro objects, such as wetted porous sheets or skin tissues, and in consequence we assume the overall diffusive character of heat transfer ($\tau_T \geq \tau_q$). The objective is to confirm and disprove this hypothesis.

2. Thermal modelling of a wire with surrounded porous material

The models with cylindrical geometry were investigated to compare the existence of the DPL phenomenon in porous materials. The first modelled object was a resistive wire. The second model includes an additional outer layer of wetted cotton wipe. In this model, the impact of dual-phase lag is assumed.

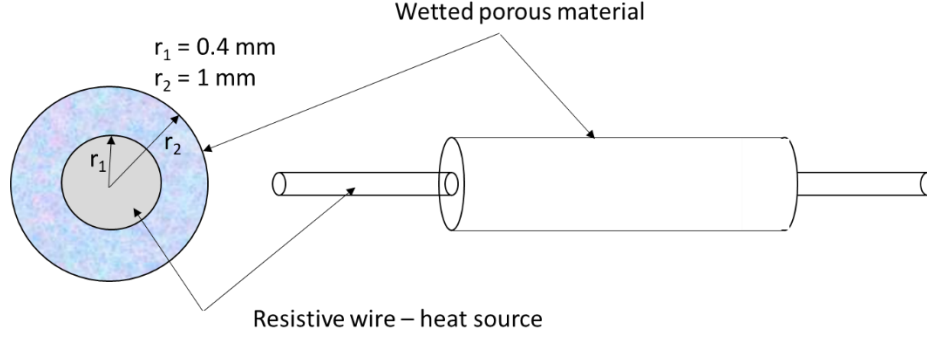


Fig. 1. Model of a wire surrounded by porous material

Assuming symmetry, the heat diffusion equation for a cylindrical object in polar coordinate system depends on radius r only and can be presented in frequency domain by the eq. (5).

$$k_i \nabla^2 T_i(r) - j\omega c_{vi} T_i(r) = -q_{vi} \quad (5)$$

where k_i is the thermal conductivity, c_{vi} the thermal capacity per volume unit, j the imaginary unit, ω the angular frequency and q_{vi} the dissipated power density in i -th layer.

General solution for the first and outer layers are below:

$$T_1(r) = A_1 I_0(b_1 r) + \frac{q_{v1}}{j\omega c_{v1}} \quad (6)$$

$$T_i(r) = A_i I_0(b_i r) + B_i K_0(b_i r) + \frac{q_{vi}}{j\omega c_{vi}} \quad (7)$$

where:

$$b_i = \sqrt{\frac{j\omega c_{vi}}{k_i}}, \quad (8)$$

and I_0 and K_0 are the modified Bessel functions of the first and second kind and order zero.

The heat source is only in the first layer – the wire. For 2-layer structure, the integration constants A_1 , A_2 and B_2 must be determined assuming the interface and boundary conditions, i.e.: continuity of temperature and heat flux between the layers. For the interface between layers 1 and 2, the equations take the following form.

$$T_1|_{r=r_1} = T_2|_{r=r_1} \quad (9)$$

$$A_1 I_0(b_1 r_1) + \frac{q_{v1}}{j\omega c_{v1}} = A_2 I_0(b_2 r_1) + B_2 K_0(b_2 r_1) \quad (10)$$

$$-k_1 \frac{dT_1}{dx} |_{r=r_1} = -k_2 \frac{dT_2}{dx} |_{r=r_1} \quad (11)$$

$$A_1 b_1 k_1 I_1(b_1 r_1) = A_2 b_2 k_2 I_1(b_2 r_1) - B_2 b_2 k_2 K_1(b_2 r_1) \quad (12)$$

At the end of the structure, convective cooling is assumed. It leads to one equation.

$$-k_2 \frac{dT_2}{dx} |_{r=r_2} = h T_2 |_{r=r_2} \quad (13)$$

$$-A_2 b_2 k_2 I_1(b_2 r_2) + B_2 b_2 k_2 K_1(b_2 r_2) = h A_2 I_0(b_2 r_2) + h B_2 K_0(b_2 r_2) \quad (14)$$

where I_1 and K_1 are the modified Bessel functions of the first and second kind and order one.

The model presented above can be analytically solved in the frequency domain. This approach significantly simplifies the calculations and leads to more general conclusions. Considering the DPL thermal model, the thermal conductivity can be considered as frequency-dependent quantity.

3. Experiment

The measurement stand consists of a functional generator and a power amplifier. The square wave signal from the generator is amplified by the transconductance driver. The output current flows through the constantan resistive wire. The square wave signal frequency varies from 1 to 20 Hz. The thermal response was measured using cooled infrared camera, the Cedip Titanium with MWIR detector of 640x512 pixel resolution. Measurements were performed to compare the thermal response of a solid body (constantan wire) with this wire surrounded by a porous material, as shown in figure 1. The wire was covered with a wetted piece of cotton material, which acts as a porous material. This cotton material effectively absorbs the water placed underneath, so it is assumed that the thermal response of such a material can exhibit the dual-phase lag. The wire was thermally excited by an amplified electrical current with frequency controlled by the functional generator. The measurements were performed for four different frequency values: 1, 2, 10, and 20 Hz. Measurement stand with the IR camera on top is presented in figure 2.

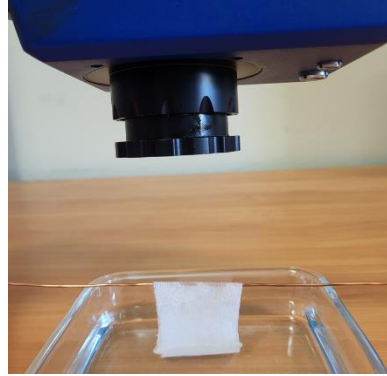


Fig. 2. Measurements stand with the high-speed IR camera

For each measurement, Fast Fourier Transform (FFT) analysis was performed. The power signal was the square wave with a DC bias, which was half of the amplitude, ensuring that the fundamental frequency both for power excitation and temperature response was the same. The measurements were carried out for the first harmonic only.

The aim of this experiment is to confirm a novel definition of thermal conductivity, which strongly depends on frequency (eq. 15).

$$k_2 = k_0 \frac{1+s\cdot\tau_T}{1+s\cdot\tau_q} \quad (15)$$

where τ_T is the delay of thermal gradient and τ_q is the delay of heat flux.

Based on the eq.(15), one can see that the conductivity of materials where DPL effect occurs, is complex and depends on frequency. This may lead to a different interpretation of non-Fourier heat transfer. Each measurement lasted 10 minutes. Frame rate of the camera was equal to $f_s = 200$ Hz.

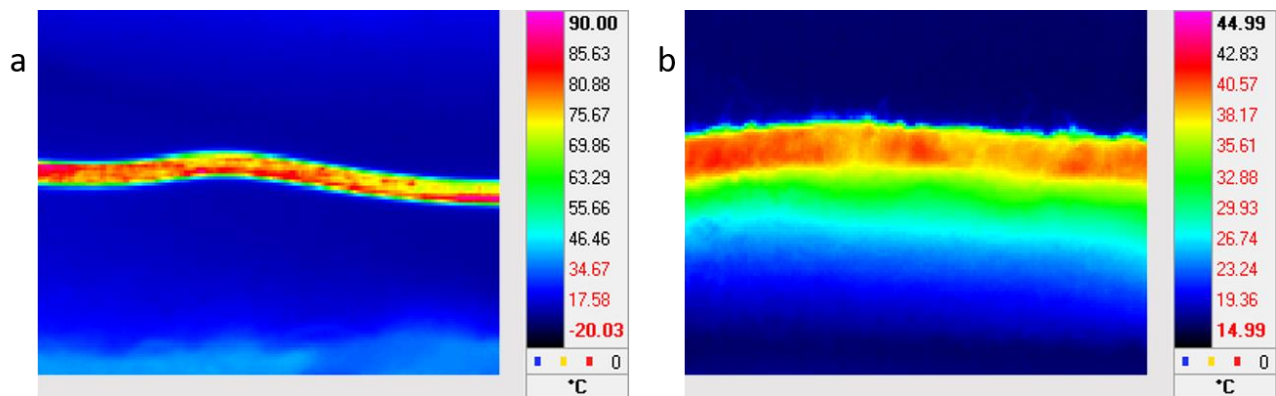


Fig. 3. Thermal image of the measured objects – wire (a), and wire with a porous material (b)

The examples of thermal images for naked wire and the wire wrapped up by wetted porous material is presented in figure 3. After registration, the Fast Fourier Transform (FFT) analysis was performed, and the amplitudes of the first harmonics were estimated for each pixel in chosen area of interest. The example of temperature vs. time generated by the IR camera and the corresponding spectrum for $f_s = 10$ Hz power excitation frequency is presented in figure 4.

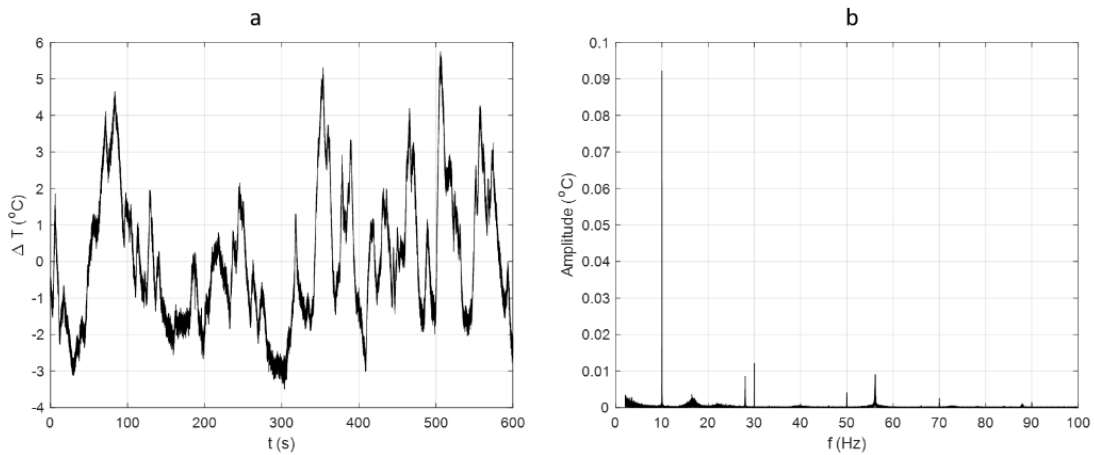


Fig. 4. Thermal response (after subtraction its mean value) of the naked wire for 10 Hz input power (a) and FFT Magnitude Spectrum of this signal (b)

Finally the map of amplitudes of temperature for different frequencies are shown in the figure 5.

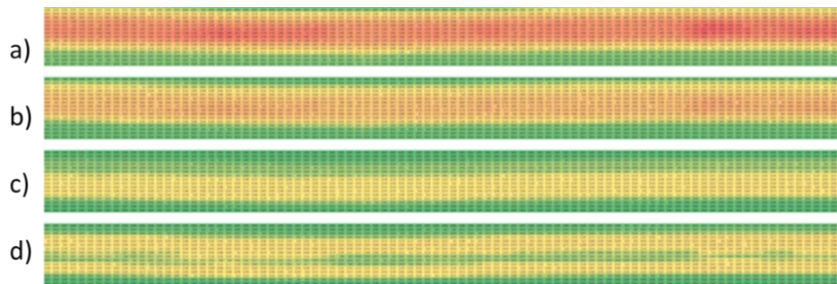


Fig. 5. Map of the temperature amplitudes measured on naked wire for different power frequency: 1 Hz (a), 2 Hz (b), 10 Hz (c), 20 Hz (d)

This research was made for the wire with porous material and for 4 frequencies (1, 2, 10, 20 Hz). Thermal images are rather non-uniform, especially for the porous material where the water content can vary in different places. The temperature was recorded for the same regions of interest in all measurements. Finally, the average temperature of 4 neighbour pixels were calculated and used for further analysis.

4. Results

The data obtained from the measurements were compared with results calculated by using the developed thermal model. The parameters of the models were adjusted to align modelling with the measurement results – table 1.

Table 1. Estimated model's parameters

Parameters	Description	Fourier-Kirchhoff model (naked wire)	DPL model, wire and wetted porous material
k_1 , W/mK	Thermal conductivity of the first layer	23	23
k_0 , W/mK	Thermal conductivity of the second layer	-	0.6
c_{v1} , J/m ³ K	Thermal capacity of the first layer	$3.6 \cdot 10^6$	$3.6 \cdot 10^6$
c_{v2} , J/m ³ K	Thermal capacity of the second layer	-	$3 \cdot 10^6$
r_1 , m	Radius of the first layer	$0.4 \cdot 10^{-3}$	$0.4 \cdot 10^{-3}$
r_2 , m	Total radius of a structure	-	$1.0 \cdot 10^{-3}$
h , W/m ² K	Heat transfer coefficient for outer surface of the second layer	20	60
q_{v1} , MW/m ³	Power density in the first layer	40	40
τ_T , s	Thermal gradient time constant	-	8
τ_q , s	Flux relaxation time constant	-	0.9

The results of Fourier-Kirchhoff model for the naked wire was fitted to the measurements. Similarly, the DPL model was tuned to the results of temperature measurements of the wire with the porous material around. Then, the objective was to confirm the impact of the existence of the DPL phenomenon. In order to achieve this goal, we model the double layer structure with and without DPL effect by zeroing the time constants τ_q and τ_T .

The Fourier-Kirchhoff model of the wire itself is one-layer model. Its parameter's values agree with those found in the literature for constantan – the resistive wire. The model of the porous material assumes existence of two layers. One layer is the same as in the first model representing the wire with the same thermal parameters. The second layer is made of cotton thin film partially filled with water, and the values of thermal conductivity and thermal capacity are very selected according the reports in literature.

For the DPL model, the thermal conductivity is complex as long as the values of temperature gradient and heat flux relaxation time constants are non-zero or are not of the same value. The chosen values (table 1) seem to be correct, as the temperature gradient time constant is higher than the flux relaxation time constant, and the ratio between them is similar to those obtained by other researchers. The high value of heat transfer coefficient h is due to evaporation of the water. Even a small amount of evaporation results in a high value of heat transfer coefficient.

The difference between the Fourier-Kirchhoff and DPL models is clearly visible in figures 6 and 7. As the Fourier – Kirchhoff model is one layer, the thermal impedance characteristic (Nyquist plot) displays the single-pole circular shape (fig. 7), resulting in a constant rate of attenuation of the Z_{th} modulus in log-log scale (fig. 6). In contrast, if we have two layers, the amplitude characteristic of Z_{th} exhibits two distinct breakpoints. This dual-pole configuration accelerates the rate of attenuation, thereby causing a more rapid decline in modulus of Z_{th} . In result, the theoretical predictions agrees with observed experimental data.

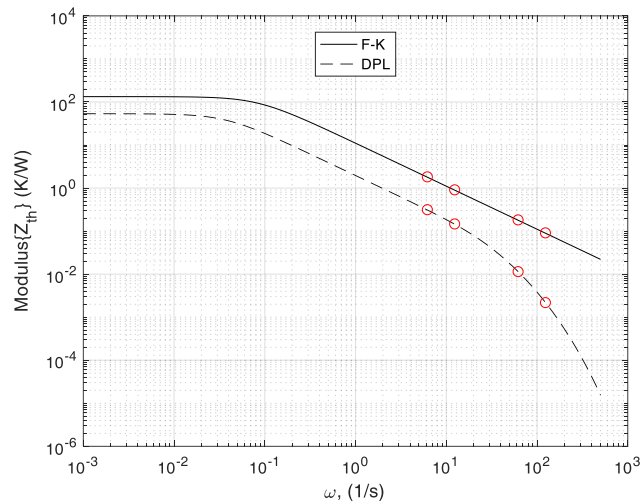


Fig. 6. Thermal impedance modulus of 5 cm long wire with wetted porous material, for Fourier-Kirchhoff model (black curve) and DPL model (dashed curve) with marked points for (1, 2, 10, 20) Hz

The Nyquist plots of thermal impedance (for a wire with wetted porous coating 5 cm long) obtained from the modelling are presented in figure 7.

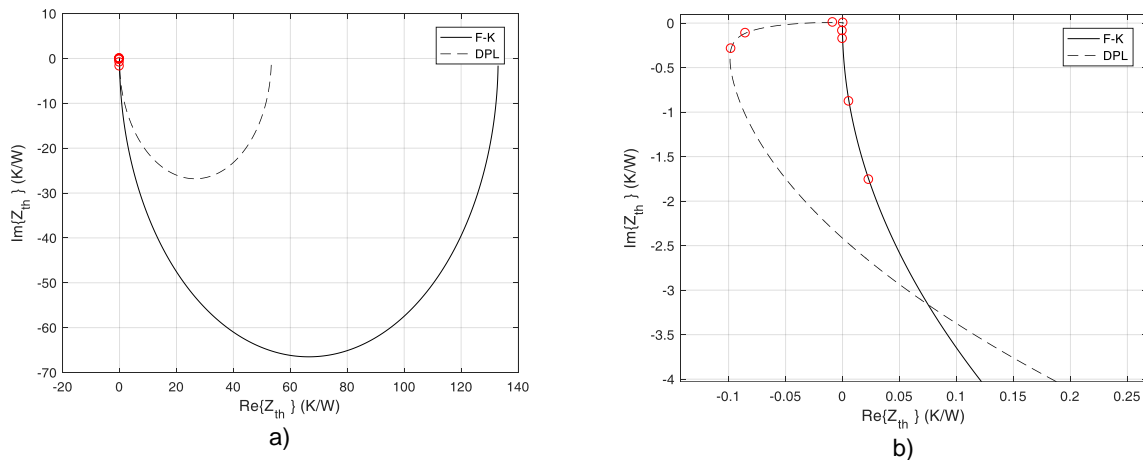


Fig. 7. Nyquist plots of F-K and DPL thermal impedance for the wire with and without wetted coating of porous material, 5 cm long (a) and zooming for high frequencies (b)

The dots on the curves indicate frequencies corresponding to the frequencies of power excitation during the measurements, specifically at 1, 2, 10 and 20 Hz. Due to the lack of phase synchronization of temperature measurements with the power variation, the amplitudes of the appropriate harmonics were considered only. After a few iteration loops we adjusted the values of model's parameters to achieve the agreement of thermal impedance measurement obtained from both model and the performed experiment for frequencies 1, 2, 10 and 20 Hz – figure 8. Since the values of Z_{th} agree, we assume that the phase shift between temperature and power can be evaluated from the model.

We also tested the model of the porous material without DPL by setting the thermal gradient and flux relaxation time constants to zero. A comparison of temperature modulus from the model of the structure with porous material with and without the DPL heat transfer effect confirm the expectations. The results show that without DPL, the modulus of temperature for a chosen frequency falls faster, while with DPL, it starts to straighten at frequency corresponding to τ_T and τ_q . This indicates the significant impact of the DPL phenomenon on the thermal behaviour of the material.

Table 2. Parameters of two layers model of the wire with porous material assuming not existing and existing DPL phenomenon

Parameters of the model	Two layers model without DPL	Two layers model with DPL in the outer layer
$k_1, W/(m \cdot K)$	23	23
$k_0, W/(m \cdot K)$	0.6	0.6
$c_{v1}, J/m^3K$	$3.6 \cdot 10^6$	$3.6 \cdot 10^6$
$c_{v2}, J/m^3K$	$3 \cdot 10^6$	$3 \cdot 10^6$
r_1, m	$0.4 \cdot 10^{-3}$	$0.4 \cdot 10^{-3}$
r_2, m	10^{-3}	10^{-3}
$h, W/m^2K$	60	60
$q_{v1}, MW/m^3$	40	40
τ_T, s	0	8
τ_q, s	0	0.9

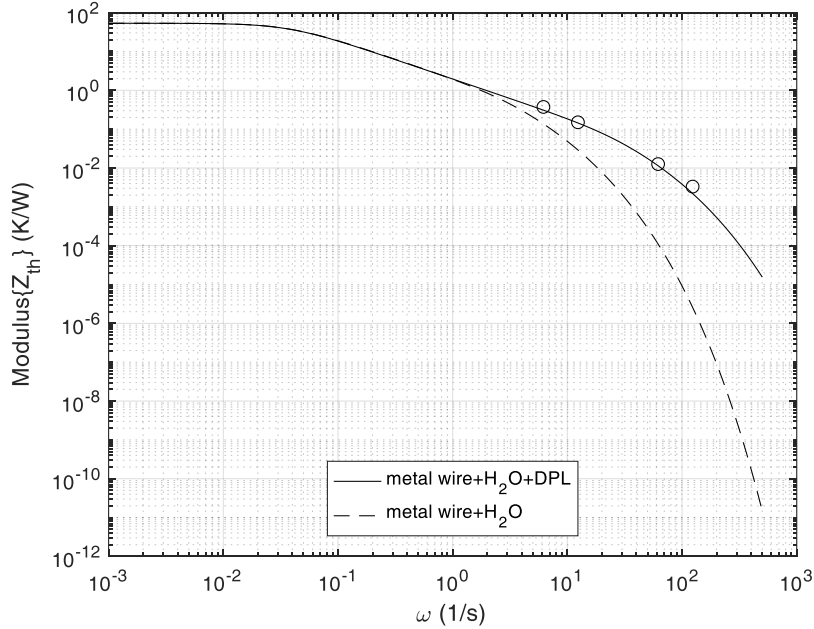


Fig. 8. Amplitude characteristics of Z_{th} for DPL model with overlapped measurement results for the wire with porous material (markers) and the same model excluding DPL effect (dashed line)

5. Conclusions

The article presents a method for analysing the thermal response of porous materials to thermal excitation and demonstrates how to confirm the existence of the dual-phase lag phenomenon in such structures. Our aim was to confirm

that the thermal conductance of these materials is a complex value that depends on the frequency of the input power signal. Based on the provided experimental and modelling results, we confirmed that this can be achieved using the presented approach by employing Fast Fourier Transform and analysing the first harmonics of the thermal response of the object. However, since this is preliminary, further experiments and improvements are necessary.

Better results can be obtained if we synchronize the input and output power signals, allowing us to consider both amplitudes and phases. This approach will provide a better understanding of the behaviour of such structures. We also plan to perform another experiment with a different setup. In this setup, the water will be absorbed by the material horizontally rather than vertically. This could result in a more uniform filling of the material with water. Nevertheless, the presented preliminary results seem promising and confirm the existence of the DPL phenomenon in porous materials.

References

- [1] Tzou D.Y., "Macro-to Microscale Heat Transfer: The Lagging Behaviour", 2nd ed., Wiley, ISBN: 978-1-118- 81822-0, 2014.
- [2] Askarizadeh, Hossein and Hossein Ahmadikia. "Extended Irreversible Thermodynamics Versus Second Law Analysis of High-Order Dual-Phase-Lag Heat Transfer." *Journal of Heat Transfer-transactions of The Asme*; 140: 082003, 2018.
- [3] Rukolaine, S. A., "Unphysical effects of the dual-phase-lag model of heat conduction: higher-order approximations," *Int. J. Therm. Sci.*; 113, pp. 83–88, 2017.
- [4] Cattaneo C., "A form of heat conduction equation which eliminates the paradox of instantaneous propagation", *Compte Rendus*; 247, pp. 431-433, 1958.
- [5] Vernotte P., "Les paradoxes de la theorie continue de l'equation de la chaleur, *Compte Rendus*"; 246, pp. 3154-3155, 1958.
- [6] B. Mochacki, M. Paruch, "Cattaneo-Vernotte Equation. Identification of Relaxation Time Using Evolutionary Algorithms", *Journal of Applied Mathematics and Computational Mechanics*; 12(4), 97-102, 2013.
- [7] E. Majchrzak, et al., "Modeling of skin tissue heating using the generalized dual phase-lag equation", *Arch. Mech.*, Vol. 67, pp. 417-437, 2015.
- [8] Zhang Y., "Generalized dual-phase lag bioheat equations based on nonequilibrium heat transfer in living biological tissues", *International Journal of Heat and Mass Transfer*, Vol. 52, pp. 4829-4834, 2009.
- [9] R. Kumar, A.K. Vashishth, and S. Ghangas, "Phase-Lag Effects in Skin Tissue during Transient Heating", *International Journal of Applied Mechanics and Engineering*, Volume 24: Issue 3, pp. 603-623, 2019.
- [10] Sunil Kumar Sharma and Dinesh Kumar, "A Study on Non-Linear DPL Model for Describing Heat Transfer in Skin Tissue during Hyperthermia Treatment", *Entropy*; 22, 481, 2020.
- [11] Dinesh Kumar, Surjan Singh, Neha Sharma, K.N. Rai, "Verified non-linear DPL model with experimental data for analyzing heat transfer in tissue during thermal therapy", *International Journal of Thermal Sciences*; 133, pp. 320-329, 2018.
- [12] Tareq Saeed, Ibrahim Abbas, "Finite element analyses of nonlinear DPL bioheat model in spherical tissues using experimental data", *Mechanics Based Design of Structures and Machines*, 15th Quantitative InfraRed Thermography Conference, Porto, Portugal, 6 – 10 July 2020.
- [13] Barletta, A., and Zanchini, E., "Hyperbolic heat conduction and local equilibrium: a second law analysis," *Int. J. Heat Mass Transf.*, 40(5), pp. 1007–1016, 1997.
- [14] Antaki, P. J., "New Interpretation of Non-Fourier Heat Conduction in Processed Meat," *J. Heat Transfer*, 127(2), pp. 189-193. DOI:10.1115/1.1844540, 2005.
- [15] M. Strąkowska, G. De Mey, B. Więcek, "Identification of the Thermal Constants of the DPL Heat Transfer Model of a Single Layer Porous Material", *Pomiary Automatyka Robotyka, Pomiary Automatyka Robotyka*, vol. 2, pp. 41-46, 2021.
- [16] M. Strakowska, G. De Mey, B. Wiecek, "Experimental verification of non-Fourier heat transfer in a multilayer skin tissue structure by IR temperature measurement", 16th Quantitative InfraRed Thermography Conference, Paris, 2022.
- [17] B. Wiecek M. Strakowska, G. De Mey, „Comparison of the Fourier-Kirchhoff, Pennes and DPL thermal models of a single layer tissue”, 15th Quantitative InfraRed Thermography Conference, Porto, 2020.
- [18] D. Jou, G. Lebon, *Extended Irreversible Thermodynamics*, Springer Dordrecht, Springer Science+Business Media B.V. 2010, <https://doi.org/10.1007/978-90-481-3074-0>